Available online at www.sciencedirect.com
SCIENCE DIRECT®
ELSEVIER
International Journal of Non-Linear Mechanics 41 (2006) 86–100
INTERNATIONAL JOURNAL OF NON-LINEAR MECHANICS
www.elsevier.com/locate/nlm

Chaotic pitch motion of an asymmetric non-rigid spacecraft with viscous drag in circular orbit

Manuel Iñarrea[a,*], Víctor Lanchares[b]

[a] Universidad de La Rioja, Área de Física Aplicada, 26006 Logroño, Spain
[b] Universidad de La Rioja, Departamento de Matemáticas y Computación, 26004 Logroño, Spain

Accepted 15 June 2005

Abstract

We study the pitch motion dynamics of an asymmetric spacecraft in circular orbit under the influence of a gravity gradient torque. The spacecraft is perturbed by a small aerodynamic drag torque proportional to the angular velocity of the body about its mass center. We also suppose that one of the moments of inertia of the spacecraft is a periodic function of time. Under both perturbations, we show that the system exhibits a transient chaotic behavior by means of the Melnikov method. This method gives us an analytical criterion for heteroclinic chaos in terms of the system parameters which is numerically contrasted. We also show that some periodic orbits survive for perturbation small enough.

Keywords: Spacecraft; Attitude dynamics; Chaos; Melnikov method

1. Introduction

The dynamics of a rotating body has been a classic topic of study in mechanics. So, in the XVIII and XIX centuries, several aspects of the motion of a rotating rigid body were studied by many authors as Euler, Cauchy, Jacobi, Poinsot, Lagrange and Kovalevskaya. Many of these theoretical results have been collected in Leimanis's book [1].

However, the study of the dynamics of rotating bodies is still very important in modern science. From a theoretical point of view, this topic offers quite interesting models and problems in the field of non-linear dynamics. In this way, the Euler's equations of motion of a rotating body are a representative example. Moreover, the dynamics of bodies in rotation have had many applications in the explanation of different physical phenomena as the motion of Earth's poles [2,3], the variation of the latitude on the surface of the Earth [4], the motion of gyrostats and gyroscopes [5], and the chaotic rotations of irregular-shaped natural satellites as Hyperion [6]. During the last decades, the interest in the dynamics of rotating bodies has considerably increased in astrodynamics and space engineering because it is an useful model to study, at first approximation, the attitude dynamics of spacecrafts and irregular-shaped natural satellites [7,8].

* Corresponding author.

0020-7462/$ - see front matter © 2005 Elsevier Ltd. All rights reserved.
doi:10.1016/j.ijnonlinmec.2005.06.010

Any spacecraft in orbit is under the action of several kinds of external disturbance torques as the solar radiation pressure, the gravity gradient torque, the magnetic torque caused by the Earth's magnetic field, or the aerodynamic torque due to the action of a resisting medium like the Earth's atmosphere [9]. Although all these external disturbances are not large in comparison with the weight of the vehicle, they cannot be considered as negligible in a closer study of the attitude dynamics of a spacecraft, because their influence may be significant in the real attitude motion of the vehicle.

The gravity gradient torque results from the variation in the gravitational force over the distributed mass of the spacecraft. This torque is related to one of the more interesting aspect in the attitude dynamics of a spacecraft: the so-called pitch motion [7]. An asymmetric satellite in closed orbit around the Earth tends to ride with its longest axis vertical, due to the effect of the gravity gradient torque. If it is deviated from this equilibrium position, the satellite would oscillate or rotate about that attitude. This kind of oscillation is sometimes called librations. In the XVIII century Euler [10], d'Alambert [11] and Lagrange [12], developed the first studies on the effect of the gravity gradient torque on the motion of celestial bodies as the Earth and the Moon. During the second part of the last century, the topic of the effects of the gravity gradient torque was revisited in relation to the determination of the spacecrafts motions. Klemperer and Baker [13], Schindler [14] and Klemperer [15], studied the librations of dumbbell and ellipsoid of revolution satellites in circular orbit. On the other hand, Moran [16] analyzed the effects of the planar librations on the orbital motion of an asymmetric satellite.

The aerodynamic drag torque is another disturbance torque that must be considered in a deeper study of the attitude dynamics of a spacecraft. In fact, there is a range of altitudes with operative satellites at which aerodynamic drag not only is not negligible but it also may even be dominant [7]. Several authors as Wainwright [17], Deimel [5], Gray [18], and other ones cited in Leimanis's book [1] have studied the dynamics of a revolving symmetric body under the influence of an aerodynamic drag. All of them assume that the action of the resisting medium surrounding the body results in a drag torque opposite to the motion and proportional to the first power of the angular velocity of the body. All these studies are also based on the premise that the rotating system is a perfectly rigid body. Unfortunately, all real materials are elastic and deformable to some degree. The model of a perfectly rigid body can lead to results not coincident with the real behavior of a spacecraft. This mistake was dramatically pointed out in 1958 when a not expected instability appeared in the rotation of the Explorer I satellite [19].

All these considerations have moved us to focus our attention in the pitch motion dynamics of an asymmetric non-rigid spacecraft in circular orbit and under the influence of an external aerodynamic drag torque. Here, non-rigid means that one of the moments of inertia is a periodic function of time. This model is a more realistic approximation to the attitude motion of a spacecraft than the perfectly rigid model, but not exempt of considerable simplifications. We also assume that the center of mass of the body is not modified. It is important to note that, due to the change in the orientation of the spacecraft in its pitch motion, the center of gravity of the satellite does not coincide, in general, with its mass center. Therefore, there is a coupling between the orbital and the libration motion of the spacecraft. However, as the vehicle is small compared to its distance to the mass center of the Earth, the deviations of the center of gravity of the spacecraft from its mass center may be considered very small. So, we also assume that there is no coupling between the orbital and pitch motion, hence the circular orbit of the spacecraft around the Earth is not affected by the libration motion. In the absence of any external torque, this system has already been studied by Lanchares et al. [20], and Iñarrea and Lanchares [21]. They analyzed and described the chaotic behavior of a dual-spin spacecraft with time-dependent moments of inertia in free motion. When an external viscous drag torque is considered Iñarrea et al. [22], studied the rotations of an asymmetric body with time dependent moments of inertia. The main contribution of the drag results in the despin of the body until it reaches an equilibrium position. However, the time dependence of the moment of inertia introduces a certain chaotic dimension in the behavior of the system in such a way that the final state of the body is in some cases unpredictable.

In the study of this kind of systems the Melnikov method proves to be a powerful tool. The Melnikov method [23] is an analytical tool to determine, at first order, the existence of homo/heteroclinic intersections and so chaotic behavior in near-integrable systems. Recently, many authors have applied the Melnikov method to reveal chaotic dynamics in several problems on rotating bodies under different kinds of perturbations. In this way, Gray et al. [24] have investigated a viscously damped free rigid body perturbed by small oscillating masses. Holmes and Marsden [25], Koiller [26], and Peng and Liu [27] have considered free gyrostats with a slightly asymmetric rotor. Tong et al. [28] have treated an asymmetric gyrostat under the uniform gravitational field. In order to study the persistence of the heteroclinic chaos in our rotating body in the presence of aerodynamic drag, we have also made use of the Melnikov method.

Despite of analytical techniques to highlight the chaotic behavior of the system, numerical computer simulations are needed to confirm the predicted behavior and give a deeper understanding on the global dynamics of the system. These simulations have been performed by means of numerical integration of the equations of motion. We have made use of several numerical tools such as, time history, Poincaré map and attractions basins. This allows us to characterize the dynamical behavior of the spacecraft pitch motion as regular or chaotic. Besides, Poincaré surfaces of section are used to reveal the existence of a stochastic layer in the absence of aerodynamic viscous drag. Finally, a comprehensive study of the final asymptotic behavior of the system is achieved focusing on the geometry of the attraction basins of the two asymptotic stable points. These all numerical features show an extremely random behavior for weak aerodynamic drag. Moreover, despite of the viscous drag, the time-periodic moment of inertia may work as a source of energy for the pitch motion. Thus, some non-decaying periodic pitch motions persist for a viscous drag small enough.

The present paper is structured in the following way. In Section 2, we describe in detail the perturbed system and we also express the equation of motion of the spacecraft pitch motion. Then we point out the main features of the phase space of the unperturbed system. In Section 3 we calculate the Melnikov function of the perturbed spacecraft. The Melnikov function yields an analytical criterion for heteroclinic chaos in terms of the system parameters. Finally, in Section 4, by means of computer numerical simulations of the spacecraft pitch motion, we use several numerical techniques to check the validity of the analytical criterion for chaos obtained through the Melnikov method. We also study in a qualitative way the chaos-order evolution of the attraction basins of the perturbed system with the strength of the aerodynamic drag.

2. Description of the system and equations of motion

Let us consider an asymmetric spacecraft with a time-dependent moment of inertia in a circular orbit with orbital angular velocity ω_o in the gravitational field of the Earth. We will make use of two different orthonormal reference frames: the orbital frame $\mathscr{R}\{O, X, Y, Z\}$ and the body frame $\mathscr{B}\{O, x, y, z\}$, both with the same origin O located at the center of mass of the spacecraft.

- The orbital frame $\mathscr{R}\{O, X, Y, Z\}$ is established with the Z-axis pointing to the mass center of the Earth O_e, the X-axis is the direction of the velocity vector of the spacecraft, and the Y-axis is normal to the orbital plane completing a right-hand orthogonal system. The base vectors of $\mathscr{R}$ are $\vec{r}_1, \vec{r}_2, \vec{r}_3$. See Fig. 1. In the usual aircraft and spacecraft terminology, the X, Y, Z axes are called, respectively, *roll*, *pitch* and *yaw* axes [7,8].
- The body frame $\mathscr{B}\{O, x, y, z\}$, is established with the directions of the axes coincident with the principal axes of the spacecraft. The base vectors of $\mathscr{B}$ are $\vec{b}_1, \vec{b}_2, \vec{b}_3$.

The relative orientation between these two reference frames results by means of three consecutive rotations involving the Euler angles (ψ, θ, ϕ). To move from the orbital axes $\{X, Y, Z\}$ to the body axes $\{x, y, z\}$, the first rotation is about the Z-axis through an angle ψ (yaw). The second rotation is about the new axis Y' by an angle θ (pitch). Finally, the third rotation is about the new axis x through an angle ϕ (roll), reaching the body axes $\{x, y, z\}$ (see Fig. 2). This particular set of Euler angles are commonly used in aircraft and spacecraft attitude and are also known as Tait–Bryan or Cardan angles [7,19,29]. We do not make use of the classical Euler angles [30] because they have a

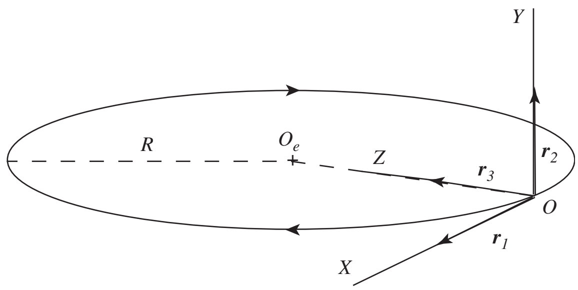

Fig. 1. The orbital reference frame $\mathscr{R}$.

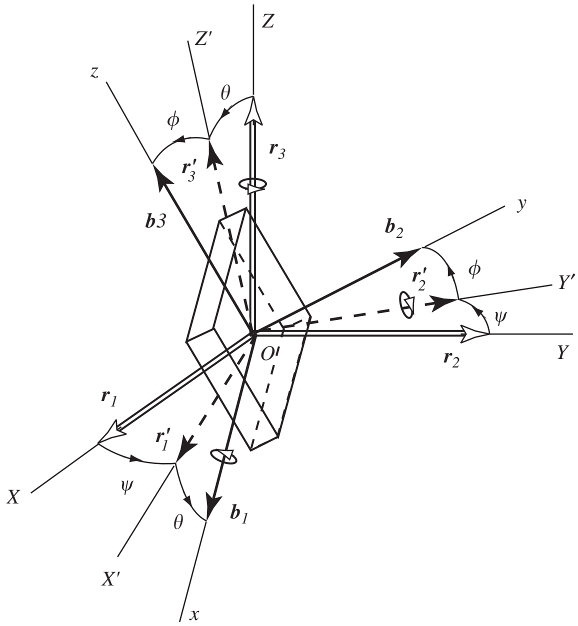

Fig. 2. The three consecutive rotations from the orbital frame $\mathscr{R}$ to the body frame $\mathscr{B}$ through the Euler yaw, pitch and roll angles (ψ, θ, ϕ).

singularity in the particular orientation that is studied in this paper.

The moments of inertia of the spacecraft are denoted by A, B, C, and we assume a triaxial spacecraft with the relation $A > B > C$. We suppose specifically that the greatest moment of inertia of the body is a periodic function of time, that is, $A = A(t)$ whereas the two other moments of inertia, B and C, remain constant. Although A varies with time, we will suppose that the body always holds the same triaxial condition, $A(t) > B > C$, at any time. Also, we will suppose that the center of mass of the body is not altered. It is important to note that the choice of the greatest moment of inertia as function of time, and the other two constant, is not relevant in the dynamics of the problem. In fact, the results and conclusions are similar if we suppose B to be variable with time and the other two constant.

The function that defines the change of the body greatest moment of inertia $A(t)$ is supposed to have the specific form

$$A(t) = A_0 + A_1 \cos \nu t, \tag{1}$$

where A_1 is a parameter much smaller than A_0 ($A_1 \ll A_0$). In this way, our system can be considered as a simple model of a non-perfectly rigid body.

Due to the gravity gradient and the finite dimension of the spacecraft, it is under the action of a gravitational torque $\vec{N}_g$ about the body mass center O. The components of this torque $\vec{N}_g$ in the body frame $\mathscr{B}$ are given by [7,8,19]

$$N_{gx} = \frac{3\mu}{R^5}(C - B)R_y R_z,$$

$$N_{gy} = \frac{3\mu}{R^5}(A - C)R_x R_z,$$

$$N_{gz} = \frac{3\mu}{R^5}(B - A)R_x R_y, \tag{2}$$

where $\mu = Gm_e = 3.986 \times 10^{14}\,\mathrm{Nm^2/kg}$ is the mass parameter of the Earth. Besides, R is the radius of the circular orbit of the spacecraft, and R_x, R_y, R_z are the components, in the body frame $\mathscr{B}$, of the position vector $\vec{R}$ of the mass center O with respect to the mass center of the Earth O_e. With our choice of the reference frames, the position vector $\vec{R}$ takes the following forms in both frames:

$$\vec{R} = R_x\vec{b}_1 + R_y\vec{b}_2 + R_z\vec{b}_3 = -R\vec{r}_3.$$

Making use of the rotation matrix from the orbital frame $\mathscr{R}$ to the body frame $\mathscr{B}$ [7,8,19], the components of $\vec{R}$ can be expressed in the body frame $\mathscr{B}$ in terms of the Euler angles as

$$R_x = R \sin \theta,$$

$$R_y = -R \sin \phi \cos \theta,$$

$$R_z = -R \cos \phi \cos \theta. \tag{3}$$

If we denote $\vec{\omega}=\omega_x\vec{b}_1+\omega_y\vec{b}_2+\omega_z\vec{b}_3$ as the rotation angular velocity of the body about its center of mass O, expressed in the body frame $\mathscr{B}$, the angular momentum $\vec{G}$ of the body about O can be written as

$$\vec{G}=\mathbb{I}\vec{\omega}=A(t)\omega_x\vec{b}_1+B\omega_y\vec{b}_2+C\omega_z\vec{b}_3,$$

where $\mathbb{I}$ is the tensor of inertia of the body. As it is expressed in the frame $\mathscr{B}$ of the principal axes of the body, this tensor is a diagonal one, that is, $\mathbb{I}=\mathrm{diag}(A(t),B,C)$.

We consider that the spacecraft is in a lightly resisting medium and its action on the body is a small drag torque $\vec{N}_\mathrm{d}$ opposite to the rotation motion about O. We also assume that the torque is directly proportional to the angular velocity $\vec{\omega}$ of the body, that is,

$$\vec{N}_\mathrm{d}=-\gamma\vec{\omega}=-\gamma(\omega_x\vec{b}_1+\omega_y\vec{b}_2+\omega_z\vec{b}_3),$$

where $\gamma>0$ is the coefficient of the viscous drag.

Under all these assumptions, and by means of the classical theorem of angular momentum about the mass center O of a body,

$$\frac{\mathrm{d}\vec{G}}{\mathrm{d}t}=\vec{N}_g+\vec{N}_\mathrm{d}.$$

Thus, the Euler equations of motion of the system, expressed in terms of the angular velocity components $(\omega_x,\omega_y,\omega_z)$, can be easily obtained

$$\begin{aligned}
&A(t)\dot{\omega}_x+\dot{A}(t)\omega_x+(C-B)\omega_y\omega_z\\
&\quad=\frac{3\mu}{R^5}(C-B)R_yR_z-\gamma\omega_x,\\
&B\dot{\omega}_y+(A(t)-C)\omega_x\omega_z\\
&\quad=\frac{3\mu}{R^5}(A(t)-C)R_xR_z-B\omega_y,\\
&C\dot{\omega}_z+(B-A(t))\omega_x\omega_y\\
&\quad=\frac{3\mu}{R^5}(B-A(t))R_xR_y-\gamma\omega_z.
\end{aligned}\tag{4}$$

As it is well known, the components $(\omega_x,\omega_y,\omega_z)$ of the angular velocity $\vec{\omega}$ in the body frame $\mathscr{B}$, can be written in terms of the Euler angles (ψ,θ,ϕ) and their velocities $(\dot{\psi},\dot{\theta},\dot{\phi})$ as [7,8,19,29]

$$\begin{aligned}
\omega_x&=\dot{\phi}-\dot{\psi}\sin\theta,\\
\omega_y&=\dot{\theta}\cos\phi+\dot{\psi}\cos\theta\sin\phi,\\
\omega_z&=\dot{\psi}\cos\theta\cos\phi-\dot{\theta}\sin\phi.
\end{aligned}\tag{5}$$

Making use of Eqs. (3) and (5) the equations of motion (4) could be explicitly written in terms of the Euler angles (ψ,θ,ϕ), their velocities $(\dot{\psi},\dot{\theta},\dot{\phi})$ and their accelerations $(\ddot{\psi},\ddot{\theta},\ddot{\phi})$, resulting in quite cumbersome expressions.

Nevertheless, if the roll and yaw motions are initially quiescent, that is, $\psi(0)=\dot{\psi}(0)=0$ and $\phi(0)=\dot{\phi}(0)=0$, the equations of motion become

$$\begin{aligned}
\ddot{\psi}&=0,\\
\ddot{\theta}&=\frac{3\omega_\mathrm{o}^2[C-A(t)]}{B}\sin\theta\cos\theta-\frac{\gamma}{B}\dot{\theta},\\
\ddot{\phi}&=0.
\end{aligned}$$

where $\omega_\mathrm{o}=\sqrt{\mu/R^3}$ is the orbital angular velocity of the spacecraft. Therefore, in this situation, roll and yaw motions are not excited by the pitch one, and there is only one non-trivial equation of motion for the dynamics of the system.

Taking into account (1), the equation of the pitch motion can be written as

$$\begin{aligned}
\ddot{\theta}=&\frac{3\omega_\mathrm{o}^2(C-A_0)}{B}\sin\theta\cos\theta-\frac{3\omega_\mathrm{o}^2A_1}{B}\\
&\times\sin\theta\cos\theta\cos(\nu t)-\frac{\gamma}{B}\dot{\theta}.
\end{aligned}$$

In order to analyze the dynamics of the pitch motion, it is convenient to introduce a new dimensionless time $\tau=\omega_\mathrm{o}t$. In this way, we arrive at the equation

$$\begin{aligned}
\ddot{\theta}=&\frac{3(C-A_0)}{B}\sin\theta\cos\theta-\frac{3A_1}{B}\\
&\times\sin\theta\cos\theta\cos\left(\frac{\nu\tau}{\omega_\mathrm{o}}\right)-\frac{\gamma}{B\omega_\mathrm{o}}\dot{\theta},
\end{aligned}$$

where the derivatives are with respect to the new dimensionless time τ. Now, by introducing the following new dimensionless parameters

$$K=\frac{3(A_0-C)}{B},\quad \varepsilon=\frac{3A_1}{B},\quad \eta=\frac{\nu}{\omega_\mathrm{o}},\quad \delta=\frac{\gamma}{B\omega_\mathrm{o}},$$

we obtain

$$\begin{aligned}
\ddot{\theta}=&-K\sin\theta\cos\theta\\
&-\varepsilon\sin\theta\cos\theta\cos(\eta\tau)-\delta\dot{\theta}.
\end{aligned}\tag{6}$$

The terms in ε and δ in Eq. (6) can be considered as small perturbations because $A_1\ll A_0$ and a small aerodynamic drag torque is supposed. In this way, the unperturbed system (ε=δ=0) coincides with an asymmetric rigid spacecraft in circular orbit under the gravity gradient torque. Thus, the equation of motion of the unperturbed spacecraft is given by

$$\ddot{\theta} = -K \sin\theta \cos\theta.$$

This equation may be rewritten in form of a system of two differential equations of first order as

$$\dot{\theta} = \omega = f_1,$$
$$\dot{\omega} = -K \sin\theta \cos\theta = f_2. \tag{7}$$

These differential equations correspond to the following Hamiltonian:

$$\mathscr{H} = \frac{1}{2} p_\theta^2 + \frac{K}{2} \sin^2\theta,$$

with $p_\theta = \omega$. In this case, the Hamilton function coincides with the sum of the rotational kinetic energy of the spacecraft about its mass center, plus the gravity gradient potential energy of the body. As it can be seen, the unperturbed spacecraft is one degree of freedom and, therefore, it is an integrable system.

Eq. (7) are those corresponding to a non-linear pendulum taking 2θ as the angular variable. Therefore, it is known that the system has unstable equilibria at $(\theta, \omega) = (\pm(2n+1)\pi/2, 0)$, and stable equilibria at $(\pm n\pi, 0)$. The two unstable equilibria, denoted by E_1 and E_2, are connected by four heteroclinic trajectories. These orbits are the separatrices of the phase space. Fig. 3 shows the main features of the phase flow for the unperturbed system (7) for $K = 1$.

The energy of the system corresponding to the unstable equilibria and the separatrices is $\mathscr{E}_{\text{sep}} = K/2$. These separatrices divide the phase space in two different classes of the pitch motion. On the one hand, oscillations inside the separatrices, when the energy of the spacecraft is $\mathscr{E} < \mathscr{E}_{\text{sep}}$,

$$\begin{aligned} \theta &= \arcsin\left[\frac{1}{k}\text{sn}\left(\sqrt{K}\tau, \frac{1}{k}\right)\right], \\ \omega &= \sqrt{2\mathscr{E}}\text{cn}\left(\sqrt{K}\tau, \frac{1}{k}\right), \end{aligned} \qquad k^2 = \frac{K}{2\mathscr{E}}, \tag{8}$$

which are periodic with period $T = \mathscr{K}(1/k)/\sqrt{K}$, being $\mathscr{K}$ the complete integral of first kind. On the other hand, tumbling rotations outside the separatrices, when the energy of the spacecraft is $\mathscr{E} > \mathscr{E}_{\text{sep}}$,

$$\begin{aligned} \theta &= \arcsin[\text{sn}(\sqrt{2\mathscr{E}}\tau, k)], \\ \omega &= \sqrt{2\mathscr{E}}\ \text{dn}(\sqrt{2\mathscr{E}}\tau, k), \end{aligned} \qquad k^2 = \frac{K}{2\mathscr{E}}, \tag{9}$$

which are periodic with period $T = \mathscr{K}(k)/\sqrt{2\mathscr{E}}$. Besides, the solutions corresponding to the four asymptotic heteroclinic trajectories are

$$\begin{aligned} [\theta^\pm(\tau), \omega^\pm(\tau)] = \{&\pm \arcsin[\tanh(\sqrt{K}\tau)], \\ &\pm\sqrt{K}\ \text{sech}(\sqrt{K}\tau)\}, \end{aligned} \tag{10}$$

subject to the initial conditions $(\theta_{\text{o}}^\pm(0), \omega_{\text{o}}^\pm(0)) = (0, \pm\sqrt{K})$. The four heteroclinic trajectories form the stable $W_{\text{s}}(E_1)$, $W_{\text{s}}(E_2)$ and unstable $W_{\text{u}}(E_1)$, $W_{\text{u}}(E_2)$ manifolds corresponding to the two unstable equilibria, that join smoothly together. So it holds that $W_{\text{s}}(E_1) = W_{\text{u}}(E_2)$ and $W_{\text{u}}(E_1) = W_{\text{s}}(E_2)$.

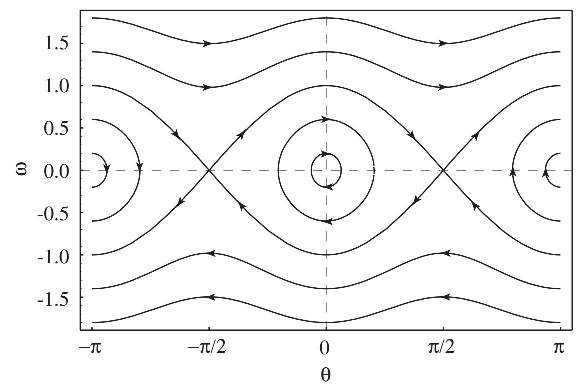

Fig. 3. The phase space of the unperturbed pitch motion of an asymmetric rigid spacecraft in circular orbit under the gravity gradient torque for $K = 1$.

3. Chaotic pitch motion. The Melnikov function

Let us consider the perturbed system. Now the stable and unstable manifolds are not forced to coincide and it is possible that they intersect transversally leading to an infinite number of new heteroclinic points. Then, a heteroclinic tangle is generated. In this case, because of the perturbation, the pitch motion of the spacecraft, near the unperturbed separatrices, becomes extremely complicated and chaotic, in the sense that the system exhibits Smale's horseshoes and a stochastic layer appears. Inside this chaotic layer small isolated regions of regular motion with periodic orbits can also appear.

The existence of heteroclinic intersections may be proved, at first order, by means of the Melnikov method [31]. In order to apply the Melnikov method, Eq. (6) is written in a more convenient form. Let us define a new parameter $\hat{\delta} = \delta/\varepsilon$, in order to consider ε as the only one small parameter of our system. In this way, Eq. (6) can be expressed as the following system of two differential equations of first order:

$$
\begin{aligned}
\dot{\theta} &= \omega = f_1 + g_1,\\
\dot{\omega} &= -K \sin\theta\cos\theta\\
&\quad - \varepsilon[\sin\theta\cos\theta\cos(\eta\tau) + \hat{\delta}\omega]\\
&= f_2 + g_2,
\end{aligned}
\tag{11}
$$

where $g_1 = 0$ and $g_2 = -\varepsilon[\sin\theta\cos\theta\cos(\eta\tau) + \hat{\delta}\omega]$.

The Melnikov function, $M^{\pm}(\tau_0)$, for system (11) is given by

$$
\begin{aligned}
&M^{\pm}(\tau_0)\\
&= \int_{-\infty}^{\infty} \vec{f}[\vec{z}^{\pm}(\tau)] \wedge \vec{g}[\vec{z}^{\pm}(\tau), \tau + \tau_0]\,\mathrm{d}\tau\\
&= \int_{-\infty}^{\infty} \{f_1[\vec{z}^{\pm}(\tau)]\; g_2[\vec{z}^{\pm}(\tau), \tau + \tau_0]\\
&\quad - f_2[\vec{z}^{\pm}(\tau)] g_1[\vec{z}^{\pm}(\tau), \tau + \tau_0]\}\,\mathrm{d}\tau\\
&= \int_{-\infty}^{\infty} f_1[\vec{z}^{\pm}(\tau)]\; g_2[\vec{z}^{\pm}(\tau), \tau + \tau_0]\,\mathrm{d}\tau\\
&= -\varepsilon \int_{-\infty}^{\infty} \omega^{\pm}(\tau)\{\sin[\theta^{\pm}(\tau)]\\
&\quad \times \cos[\theta^{\pm}(\tau)]\cos[\eta(\tau + \tau_0)]\\
&\quad + \hat{\delta}\omega^{\pm}(\tau)\}\,\mathrm{d}\tau,
\end{aligned}
\tag{12}
$$

where $\vec{z}^{\pm}(\tau) = (\theta^{\pm}(\tau), \omega^{\pm}(\tau))$ are precisely the solutions of the unperturbed heteroclinic orbits (10).

The Melnikov function $M^{\pm}(\tau_0)$ give us a measure of the distance between the stable and unstable manifolds of the perturbed hyperbolic fixed points. Thus, if $M^{\pm}(\tau_0) = 0$ there are transverse intersections between the stable and unstable trajectories.

Now, by substitution of Eqs. (10) into (12) we obtain, for the positive branch of the Melnikov function,

$$
\begin{aligned}
M(\tau_0) &= M_1 + M_2\\
&= -\varepsilon\sqrt{K}\int_{-\infty}^{\infty} \operatorname{sech}^2(\sqrt{K}\tau)\\
&\quad \times \tanh(\sqrt{K}\tau)\cos[\eta(\tau + \tau_0)]\,\mathrm{d}\tau\\
&\quad - \varepsilon\hat{\delta}K\int_{-\infty}^{\infty} \operatorname{sech}^2(\sqrt{K}\tau)\,\mathrm{d}\tau,
\end{aligned}
\tag{13}
$$

being M_1 and M_2 the Melnikov functions corresponding to both perturbations: the time-dependent moment of inertia and the aerodynamic viscous drag, respectively.

To compute the first term $M_1(\tau_0)$ the Cauchy's residue theorem can be used. However, after integrating by parts we arrive at an integral that is tabulated in [32]. In this way, we obtain

$$
\begin{aligned}
M_1(\tau_0) &= \frac{\pi\varepsilon\eta^2}{2K}\operatorname{cosech}\left(\frac{\pi\eta}{2\sqrt{K}}\right)\sin(\eta\tau_0)\\
&= M_{1\,\max}\sin(\eta\tau_0),
\end{aligned}
\tag{14}
$$

where $M_{1\,\max}$ represent a good measure of the maximum splitting of the stable and unstable manifolds when the spacecraft is only under the action of the first perturbation: the time-dependent moment of inertia.

The second integral M_2 yields directly

$$
\begin{aligned}
M_2 &= -\varepsilon\hat{\delta}K\int_{-\infty}^{\infty} \operatorname{sech}^2(\sqrt{K}\tau)\,\mathrm{d}\tau\\
&= -2\varepsilon\hat{\delta}\sqrt{K}.
\end{aligned}
\tag{15}
$$

Thus, the complete Melnikov function $M(\tau_0)$ results in

$$
\begin{aligned}
M(\tau_0) &= M_1 + M_2\\
&= \varepsilon\left[\frac{\pi\eta^2}{2K}\operatorname{cosech}\left(\frac{\pi\eta}{2\sqrt{K}}\right)\right.\\
&\quad \left.\times \sin(\eta\tau_0) - 2\hat{\delta}\sqrt{K}\right].
\end{aligned}
\tag{16}
$$

It is important to note that Eq. (16) give us an analytical criterion for heteroclinic chaos in terms of the system parameters. Indeed, from (16) it is easy to derive that the Melnikov function $M(\tau_0)$ has simple zeros for

$$
\hat{\delta} < \hat{\delta}_c = \frac{\pi\eta^2}{4\sqrt{K^3}}\operatorname{cosech}\left(\frac{\pi\eta}{2\sqrt{K}}\right).
\tag{17}
$$

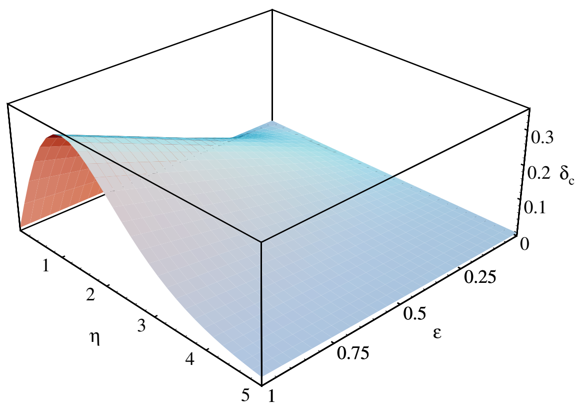

Fig. 4. Three-dimensional plot of the critical value δ_c versus the amplitude ε and the frequency η for $K = 1$.

Thus, for $\hat{\delta} < \hat{\delta}_c$ the perturbations produce heteroclinic intersections between the stable and unstable manifolds of the hyperbolic equilibria E_1 and E_2, and therefore chaotic behavior near the unperturbed separatrix. On the other hand, for $\hat{\delta} > \hat{\delta}_c$, the Melnikov function $M(\tau_0)$ is bounded away from zero, and hence there are no heteroclinic intersections and no chaos in the pitch motion of the perturbed spacecraft.

Taking into account that $\hat{\delta} = \delta/\varepsilon$, the analytical criterion (17) for chaotic behavior can be expressed in terms of δ, ε and η as

$$\delta < \delta_c = \frac{\pi\varepsilon\eta^2}{4\sqrt{K^3}} \operatorname{cosech}\left(\frac{\pi\eta}{2\sqrt{K}}\right). \tag{18}$$

It is worth to note that the critical value δ_c is directly proportional to the maximum width of the stochastic layer $M_{1\,\max}$ in the absence of external viscous drag, see (14). In this way, δ_c can be written as

$$\delta_c = \frac{1}{2\sqrt{K}} M_{1\,\max}.$$

This fact proves that the wider the layer a stronger drag is necessary to eliminate the chaotic pitch motion.

In Fig. 4 we show a three-dimensional plot of the critical value δ_c versus the parameters ε and η for $K = 1$. It can be observed, according to Eq. (18), that, fixed the frequency η, the critical value δ_c is a linear function of the amplitude ε. On the other hand, keeping ε constant and varying the frequency η we see that δ_c grows, as a function of v, until it reaches a maximum value and then decreases asymptotically to zero. In fact, we can observe that δ_c goes to 0 as $\eta \to 0$ or $\eta \to \infty$, that is to say, this two limit cases are regular limits for the pitch motion of the perturbed spacecraft.

4. Numerical analyses

In order to check the validity of the analytical criterion given by (18), several numerical techniques are used. They are based on the numerical integration of the equations of motion (11) by means of a Runge–Kutta algorithm of fifth order with fixed step [33].

Firstly, we have analyzed the evolution of the dynamical behavior of the spacecraft as the system parameters vary, studying the time histories of the angle θ, the Poincaré surfaces of section and the power spectra of several trajectories. To this end, we have used appropriate algorithms [34,35] implemented with the symbolic manipulator MATHEMATICA [36]. The Poincaré surfaces of section consist of time sections $t = \text{cte.}(\text{mod } T)$ of the three-dimensional (θ, ω, t) extended phase space.

Fig. 5 shows the numerical simulations of the same trajectory with initial conditions close to the unperturbed separatrix $(\theta_o, \omega_o) = (0, 0.999)$ for the unperturbed spacecraft (left column), and for the time-dependent moment of inertia spacecraft ($K = \eta = 1$, $\varepsilon = 0.1$) without drag ($\delta = 0$) (right column). In this figure, we can see clearly how the regular trajectory in the unperturbed system becomes a chaotic one when the greatest moment of inertia varies. This transformation is confirmed in the right column by the irregular time evolution of pitch angle θ (a) which turns into a complex trajectory in the phase space (b) where oscillations and tumbling rotations alternate in an irregular order. The Poincaré map (c) also shows how this orbit lies mainly in the stochastic layer around the unperturbed separatrix. Finally, the broadly distributed power spectrum (d) gives another sign of the chaotic behavior of the orbit.

The effect of the viscous drag in the dynamical behavior of the spacecraft is shown in Fig. 6. This figure depicts the numerical simulations of the same trajectory with initial conditions near the unperturbed separatrix $(\theta_o, \omega_o) = (-\pi/2, 0.001)$ for a small drag, $\delta = 0.001$ (left column), and for a bigger drag, $\delta = 0.01$

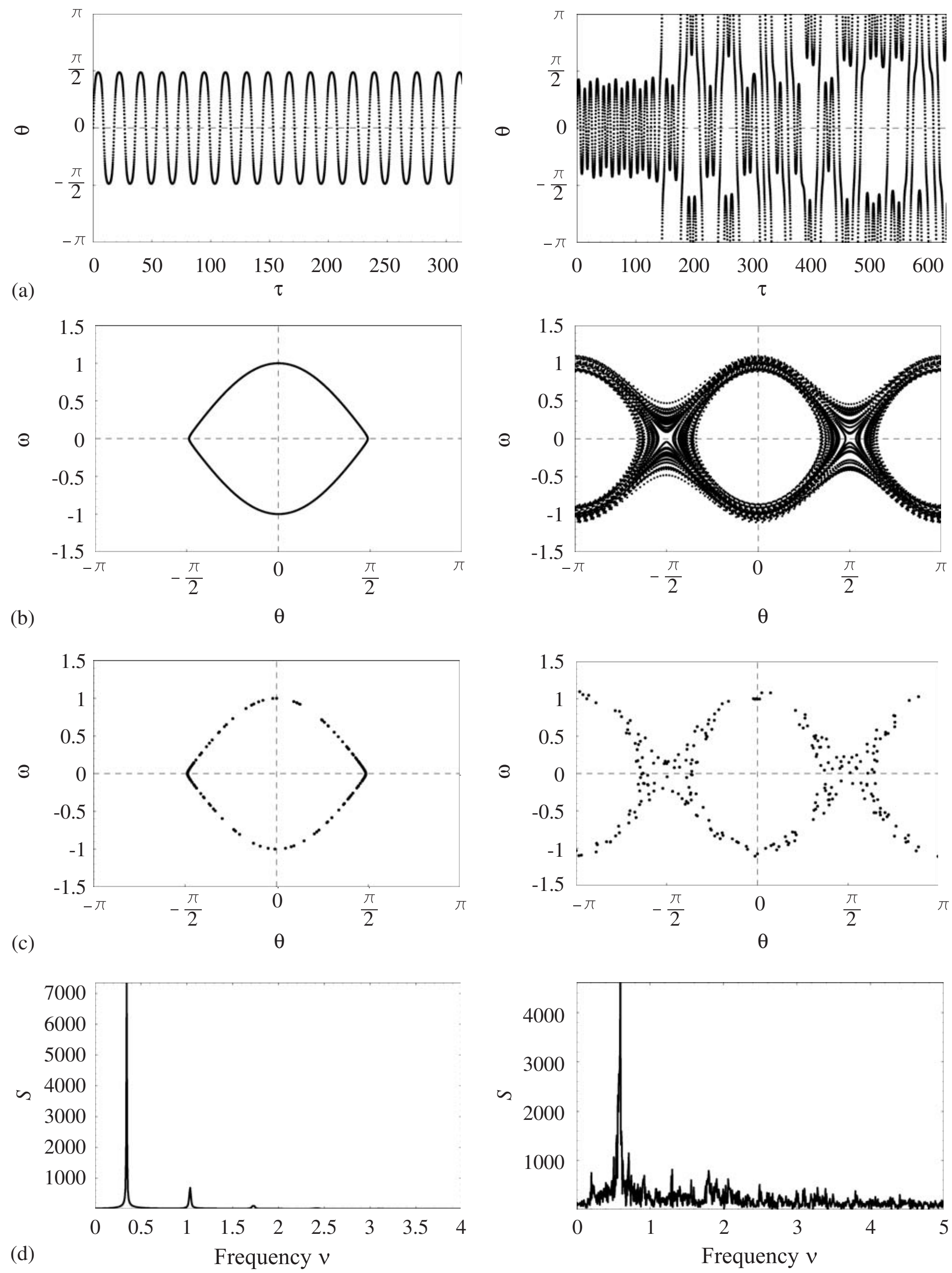

Fig. 5. Numerical simulation of the pitch motion for a single initial condition near the unperturbed separatrix $(\theta_o, \omega_o) = (0, 0.999)$. Left column: unperturbed spacecraft ($K = \eta = 1$, $\varepsilon = \delta = 0$). Right column: spacecraft perturbed with time-dependent moment of inertia and without drag ($K = \eta = 1$, $\varepsilon = 0.1$, $\delta = 0$). (a) Time evolution of angle θ. (b) Trajectory in the phase space. (c) Poincaré surface of section. (d) Power spectrum.

(right column), keeping constant the rest of the system parameters, $K = \eta = 1$, $\varepsilon = 0.1$. It can be observed that for small drag, trajectories starting close to the unperturbed separatrix exhibit an initial long transient chaotic regime and then a slow decay to an attracting fixed equilibrium, $(0, 0)$ or $(\pm\pi, 0)$. That transient

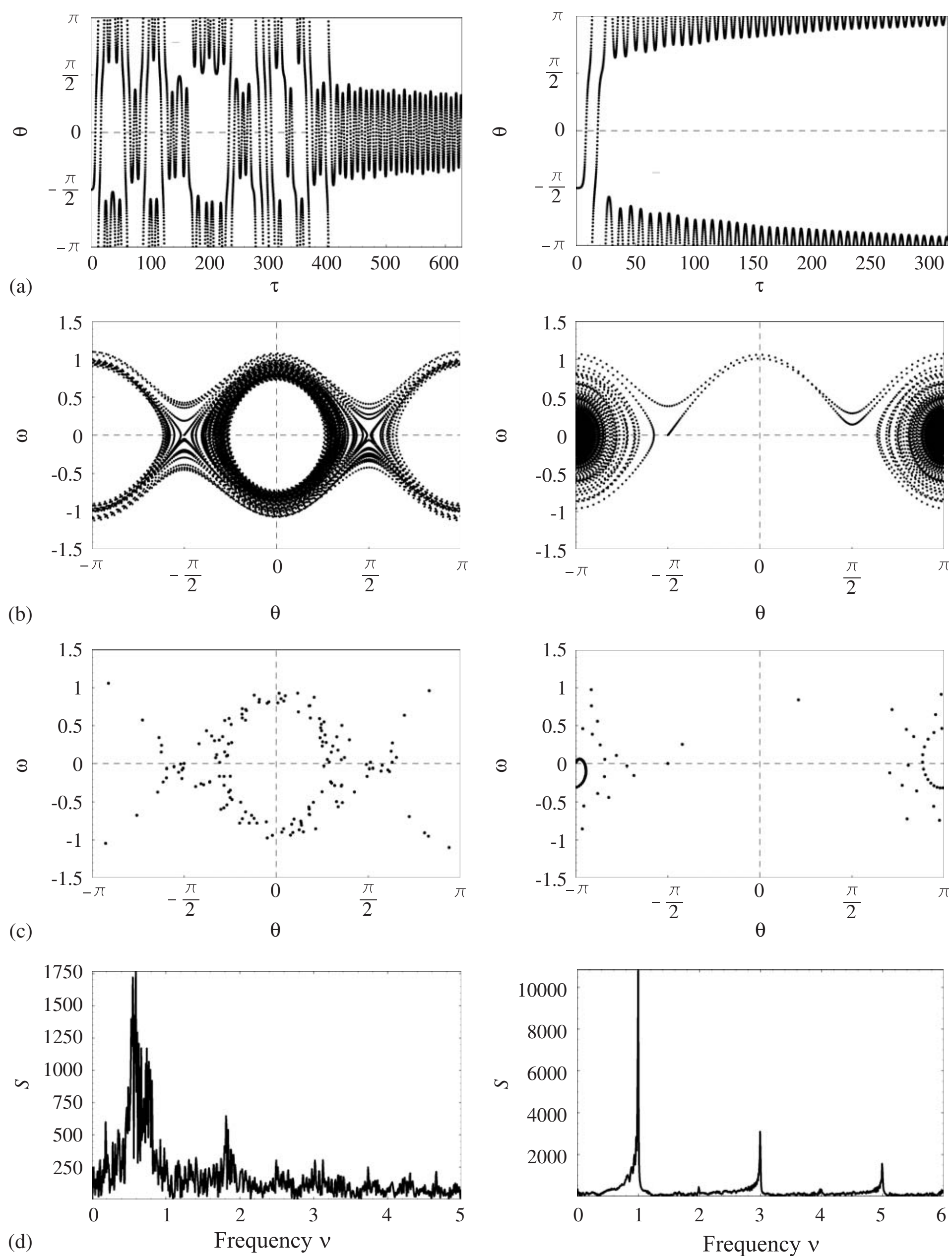

Fig. 6. Numerical simulation of the pitch motion of the spacecraft under both perturbations ($K = \eta = 1, \varepsilon = 0.1, \delta \neq 0$) for a single initial condition close to the unperturbed separatrix $(\theta_o, \omega_o) = (-\pi/2, 0.001)$. Left column: small drag $\delta = 0.001$. Right column: greater drag $\delta = 0.01$. (a) Time evolution of angle θ. (b) Trajectory in the phase space. (c) Poincaré surface of section. (d) Power spectrum.

chaotic regime generates the corresponding transient stochastic layer in the Poincaré surface of section (c) and the broadly distributed power spectrum (d). Nevertheless, the bigger the drag the shorter the transient chaotic regime. In this way, for big drags, the trajectory becomes a regular one decaying to an attracting fixed point. It is confirmed by the disappearance of the stochastic layer in the phase space (c) and the simple neat peaked power spectrum (d).

Therefore, for fixed parameters K, η, and ε, the dynamical behavior of the spacecraft near the unperturbed separatrix suffers a transition from a chaotic regime to a regular one, when the viscous drag parameter δ is increased. This transition from chaos to order is in a qualitative good agreement with the analytical criterion (18) obtained from the Melnikov method in the previous section.

In order to check in a quantitative way the validity of the analytical criterion (18) we focus on the evolution of the stable $W_s(E_i)$ and unstable $W_u(E_i)$ manifolds associated to the saddle fixed points E_1, E_2 of the Poincaré map as a function of the drag parameter δ. We have numerically calculated the invariant manifolds with the commercial software DYNAMICS [37]. Fixing the parameters $K=\eta=1$, $\varepsilon=0.1$ Eq. (18) gives a critical drag parameter $\delta_c \approx 0.0341285$. Now, we tune δ from values less than δ_c to greater ones (see Fig. 7). It can be observed clearly that, for $\delta < \delta_c$ ($\delta=0.03$), the stable and unstable manifolds transversally intersect each other (7(a)). However, when $\delta > \delta_c$ ($\delta = 0.04$), the invariant manifolds do not intersect (7(c)). Finally, Fig. 7(b) shows just the situation for the critical value δ_c, where it can be seen the tangency of the stable and unstable manifolds. This description, based on numerical simulations for concrete parameter values, is in very good agreement with the analytical criterion (18) provided by the Melnikov method.

Both numerical and analytical studies show, with very good agreement, the existence of transient chaotic behavior for given values of the parameters K, ε and η despite of $\delta < \delta_c$. This chaotic behavior is not only reflected in the existence of irregular oscillations and tumbling rotations alternated in a random way near the unperturbed separatrix. The chaotic dynamical feature of the system is also reflected, as we will see, in a very random asymptotic behavior. As it is well known, the main contribution of the viscous drag in a dynamical system is opposing the motion of the system. So, it is expected that it does not matter the initial conditions are, the oscillations and rotations of the pitch motion will decay, and the final state of the spacecraft will be with a constant pitch angle $\theta = 0$ or $\theta = \pi$. That is to say, the two fixed equilibria located at $(\theta_o, \omega_o)=(0, 0)$ or $(\pi, 0)$ are two sinks for the system. However, not all trajectories will end in an equilibrium position; some periodic orbits of period $T=2\pi n/\eta$, $n \in \mathbf{N}$, will survive for perturbations small enough [38].

We focus on the geometry of attraction basins of the two sinks depending on the parameters of the spacecraft. In this way, for given values of K, ε and η, we tune δ from the chaotic regime ($\delta < \delta_c$) to the regular one ($\delta > \delta_c$) with the aim to detect changes in the geometrical structure of the basins. To this end, a two-dimensional grid of initial conditions (θ, ω) with steps of 0.02, has been considered. The trajectories corresponding to each one of these initial conditions have been numerically integrated in order to know its w-limit point. This grid is transformed into a binary matrix depending on the corresponding w-limit point of each initial conditions. The resulting matrix is submitted as input to the commercial software TRANSFORM [39] which produces the pictures in Fig. 8 by assigning the same colors (black or white) to the same values of the matrix.

Fig. 8 shows how the basins look like as δ varies from the chaotic regime to the regular one. We note that for regular behavior the two attraction basins are well defined and separated by smooth curves in phase plane. Thus, given an initial condition, it is possible to decide the w-limit point of the trajectory through it, that is, the final state of the spacecraft. On the contrary, for chaotic behavior the attraction basins are no longer well defined and we find areas where the two basins merge. These mixing areas are bigger as the chaotic behavior increases, that is, for small values of δ.

Note that the basins are mainly destroyed outside the separatrix while inside it two well-defined basins remain. This fact is owing to the different nature of the trajectories inside and outside of the separatrix. Inside orbits are not affected by heteroclinic chaos except those orbits that initially lie on the stochastic layer. On the other hand, outside trajectories necessarily have to cross this stochastic layer to reach one of the two attractors. So, the longer the time the trajectory spends in chaotic regime (surrounding the separatrix inside the stochastic layer) the more the uncertainty to know the final state. Thus, for small values of δ the points of the attraction basin of each of the two sinks are distributed at random outside the separatrix as well along the stochastic layer, as it can be seen in Fig. 8(a) and (b). We also note that the figures are symmetric with respect to the origin. This is a consequence of the

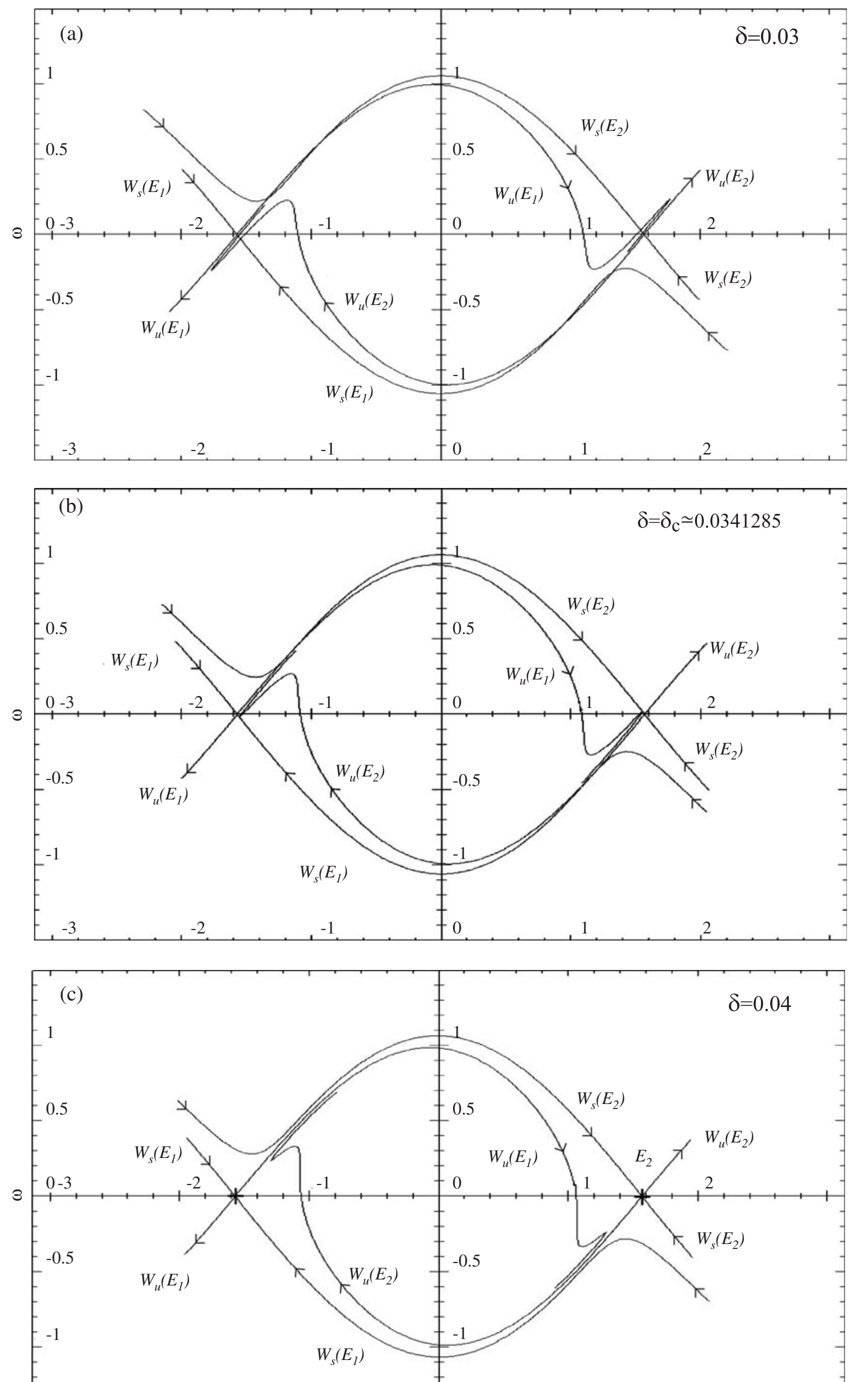

Fig. 7. Evolution of the stable and unstable manifolds as a function of δ for $K = \eta = 1$, $\varepsilon = 0.1$ and three different values of δ close to the critical value δ_c. (a) $\delta = 0.3$. (b) $\delta = 0.0341285 \approx \delta_c$. (c) $\delta = 0.4$.

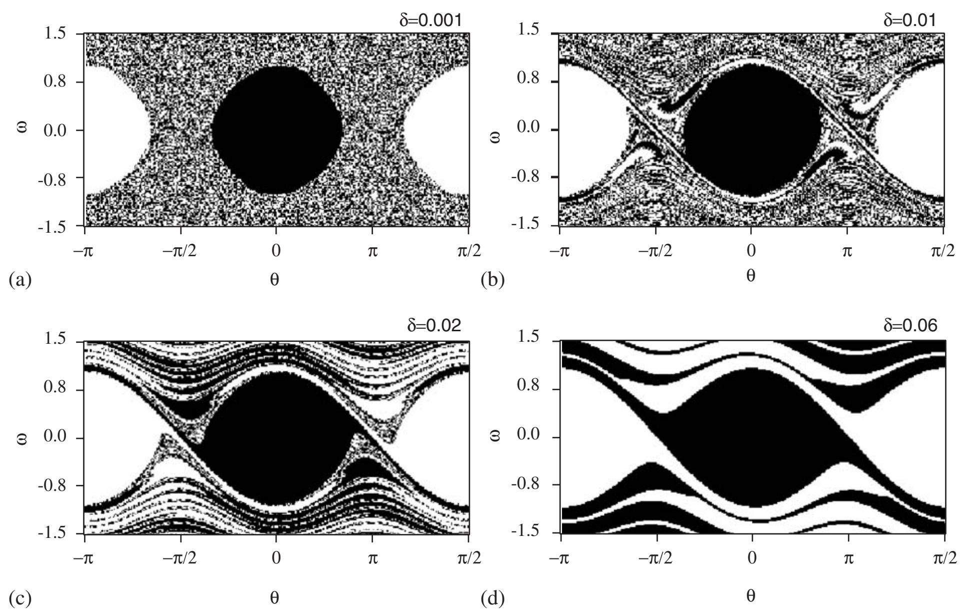

Fig. 8. Evolution of the geometric structure of the attraction basins as a function of δ for $K = \eta = 1$ and $\varepsilon = 0.1$. In white, regions of initial conditions tending to $(\pm\pi, 0)$. Black color stands for initial conditions tending to $(0, 0)$. In gray, other initial conditions.

discrete symmetry of Eq. (11). Indeed, if $(\theta(\tau), \omega(\tau))$ is a solution, $(-\theta(\tau), -\omega(\tau))$ is also a solution with the same asymptotic behavior.

As we mentioned above, not all initial conditions correspond to trajectories decaying to the w-limit points $(0, 0)$ or $(\pi, 0)$. In fact, for certain parameter values there are some few initial conditions that correspond to non-decaying periodic pitch motions of oscillation or tumbling rotation. Some of this special initial conditions can be hardly seen depicted in gray in Fig. 8(c) for $\delta = 0.02$. They are close to the $2\pi n/\eta$ periodic orbits of the unperturbed problem.

Fig. 9 shows the time history, trajectory, Poincaré surface of section and power spectrum of one of these periodic pitch motions with initial condition $(\theta_o, \omega_o) = (-1.38159, 0.1)$ for the parameter values $(K = \eta = 1, \varepsilon = 0.1, \delta = 0.02)$. In Fig. 9(c) and (d) may be observed that the frequency $v = 0.5$ of this periodic trajectory is half of the frequency $\eta = 1$ of the time-dependent perturbation. Fig. 9(b) also shows, plotted in dashed line, the periodic trajectory of frequency $v = 0.5$ corresponding to the unperturbed problem. It can be seen that both trajectories almost coincide and therefore, this particular periodic pitch oscillation is practically not affected by the perturbations.

At first, the existence of these periodic pitch motions under a viscous drag may seem paradoxical, as the drag produces a dissipation of the energy. Nevertheless, the other perturbation on the spacecraft, the time-periodic moment of inertia, may work as a source of energy, depending on the frequency of the perturbation and the natural frequency of the oscillation or rotation of the unperturbed pitch motion. This source of energy is due to the extra gravity gradient torque resulting from the variation of the moment of inertia. In this way, those periodic pitch motions, as the one shown in Fig. 9, that persist under the viscous drag, are determined by a balance between the energy added by the time-dependent moment of inertia perturbation and the energy dissipated by the viscous drag. The phenomenon of the existence of periodic motions under viscous drag also appears in the well-known problem of the driven damped simple pendulum [40].

5. Conclusions

The pitch motion dynamics of an asymmetric spacecraft in circular orbit subject to a gravity gradient

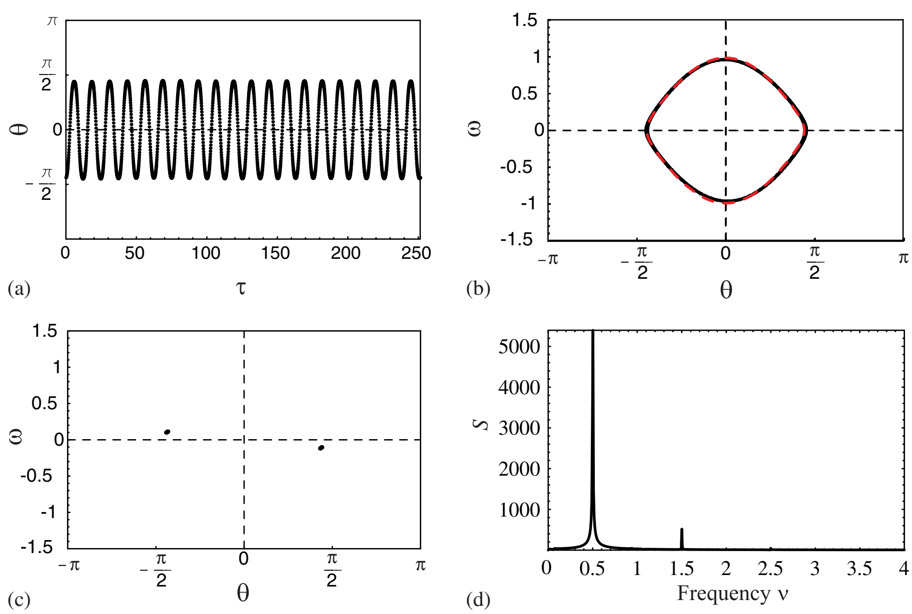

Fig. 9. Numerical simulation of a periodic not dumped pitch oscillation of the spacecraft under both perturbations ($K=\eta=1$, $\varepsilon=0.1$, $\delta=0.02$) with initial condition $(\theta_o, \omega_o) = (-1.38159, 0.1)$. (a) Time evolution of angle θ. (b) Trajectory in the phase space. In dashed line the non-perturbed trajectory with same frequency. (c) Poincaré surface of section. (d) Power spectrum.

torque has been studied. The system is perturbed by an aerodynamic viscous drag and a time-dependent periodic moment of inertia.

We have established the existence of transient heteroclinic chaos by means of the Melnikov method. Moreover, this method has provided an analytical criterion for the existence of chaotic behavior in terms of the system parameters. We have found a transition from chaotic to regular regime in the pitch motion of the spacecraft, as the heteroclinic chaos can be removed by increasing the viscous drag.

In addition, we have also investigated numerically the pitch motion dynamics by using several tools based on computer simulations, including time history, Poincaré map, power spectrum and attraction basins. In these numerical studies, we have found the persistency of some non-decaying periodic pitch motions in the perturbed system. This persistency may be explained as a consequence of a balance between the addition and dissipation of energy produced by both perturbations. The analytical results given by the Melnikov method have been confirmed with very good agreement by this numerical research.

Acknowledgements

This work has been partially supported by Project # BFM2002-03157 of Ministerio de Ciencia y Tecnología (Spain), Project # ACPI2002/04 of Departamento de Educación y Cultura, Gobierno de La Rioja (Spain), Project # API02/20 of Universidad de La Rioja (Spain) and Project Resolución 92/2002 of Departamento de Educación y Cultura, Gobierno de Navarra (Spain).

References

[1] E. Leimanis, The General Problem of the Motion of Coupled Rigid Bodies about a Fixed Point, Springer, Berlin, 1965.
[2] G. Peano, Sopra lo spostamento del polo sulla terra, Atti. R. Accad. Sci. Torino. 30 (1895) 515–523.
[3] G. Peano, Sul moto del polo terrestre, Atti. R. Accad. Sci. Torino. 30 (1895) 845–852.
[4] V. Volterra, Sur la théorie des variations des latitudes, Acta Math. 22 (1899) 201–358.
[5] R.F. Deimel, Mechanics of the Gyroscope. The Dynamics of Rotation, second ed., Dover, New York, 1952.
[6] J. Wisdom, J. Peale, R. Mignard, Chaotic rotation of hyperion, Icarus 58 (1984) 137–152.

[7] P.C. Hughes, Spacecraft Attitude Dynamics, Wiley, New York, 1986.
[8] M.J. Sidi, Spacecraft Dynamics and Control, Cambridge University Press, New York, 1997.
[9] A.E. Bryson, Control of Spacecraft and Aircraft, Princeton University Press, Princeton, 1994.
[10] L. Euler, Reserches sur la précession des équinoxes et sur la nutation de l'axe de la terre, Mem. Acad. Sci. Berlin (1749) 289–325.
[11] J. le R. d'Alambert, Reserches sur la précession des équinoxes, et sur la nutation de l'axe de la terre, dans la'hypothèse de la dissimilitude des méridiens, Mem. Acad. Sci. Paris (1759) 413–428.
[12] J.E.L. Lagrange, Théorie de la libération de la lune, et des autres phénomènes qui dépendent de la figure non sphérique de cette planète, Nouv. Acad. Sci. Berlin (1780) 203–309.
[13] W.B. Klemperer, R.M. Baker Jr., Satellite libration, Astronaut. Acta 3 (1956) 16–27.
[14] G.M. Schindler, On satellite librations, ARS J. 29 (1959) 368–370.
[15] W.B. Klemperer, Satellite librations of large amplitude, ARS J. 30 (1960) 123–124.
[16] J.P. Moran, Effect of plane librations on the orbital motion of a dumbell satellite, ARS J. 31 (1961) 1089–1096.
[17] L. Wainwright, On damping effects in exterior ballistics, Philos. Mag. 3 (1927) 641–660.
[18] A. Gray, A Treatise on Gyrostatics and Rotational Motion, Dover, New York, 1959.
[19] W.E. Wiesel, Spaceflight Dynamics, second ed., McGraw-Hill, New York, 1997.
[20] V. Lanchares, M. Iñarrea, J.P. Salas, Spin rotor stabilization of a dual-spin spacecraft with time dependent moments of inertia, Int. J. Bifurcation Chaos 8 (1998) 609–617.
[21] M. Iñarrea, V. Lanchares, Chaos in the reorientation process of a dual-spin spacecraft with time-dependent moments of inertia, Int. J. Bifurcation Chaos 10 (2000) 997–1018.
[22] M. Iñarrea, V. Lanchares, V.M. Rothos, J.P. Salas, Chaotic rotations of an asymmetric body with time-dependent moments of inertia and viscous drag, Int. J. Bifurcation Chaos 13 (2003) 393–409.
[23] V.K. Melnikov, On the stability of the center for time periodic perturbations, Trans. Moscow Math. Soc. 12 (1963) 1–56.
[24] G.L. Gray, D.C. Kammer, I. Dobson, A.J. Miller, Heteroclinic bifurcations in rigid bodies containing internally moving parts and a viscous damper, J. Appl. Mech.-Trans. ASME 66 (1999) 720–728.
[25] P.J. Holmes, J.E. Marsden, Horseshoes and Arnold diffusion for Hamiltonian systems on Lie groups, Indiana Univ. Math. J. 32 (1983) 273–309.
[26] J. Koiller, A mechanical system with a "wild" horseshoe, J. Math. Phys. 25 (1984) 1599–1604.
[27] J. Peng, Y. Liu, Chaotic motion of a gyrostat with asymmetric rotor, Int. J. Non-Linear Mech. 35 (2000) 431–437.
[28] X. Tong, B. Tabarrok, F.P.J. Rimrott, Chaotic motion of an asymmetric gyrostat in the gravitation field, Int. J. Non-Linear Mech. 30 (1995) 191–203.
[29] F.J. Hale, Introduction to Space Flight, Prentice-Hall, Englewood Cliffs, NJ, 1994.
[30] H. Goldstein, C.P. Poole, J.L. Safko, Classical Mechanics, third ed., Pearson, Upper Saddle River, 2001.
[31] J. Guckenheimer, P. Holmes, Nonlinear Oscillations, Dynamical Systems and Bifurcations of Vector Fields, Springer, New York, 1983.
[32] I.S. Gradshteyn, I.M. Ryzhik, Table of Integrals, Series and Products, Academic Press, San Diego, 1980.
[33] J.D. Lambert, Computational Methods in Ordinary Differential Equations, Wiley, London, 1976.
[34] P.T. Tam, A Physicist's Guide to Mathematica, Academic Press, San Diego, 1997.
[35] R.H. Enns, G.C. McGuire, Nonlinear Physics with Mathematica for Scientists and Engineers, Birkhäuser, Boston, 2001.
[36] S. Wolfram, The Mathematica Book, fourth ed., Cambridge University Press, Cambridge, 1999.
[37] H.E. Nusse, J.A. Yorke, Dynamics: Numerical Explorations, second ed., Spinger, New York, 1998.
[38] E.A. Coddington, N. Levinson, Theory of Ordinary Differential Equations, McGraw-Hill, New York, 1955.
[39] Fortner Research LLC, TRANSFORM, Sterling, 1996.
[40] N.J. Giordano, Computational Physics, Prentice-Hall, Upper Saddle River, 1997.